

UCRL-CONF-231744



LAWRENCE
LIVERMORE
NATIONAL
LABORATORY

Injector particle simulation and beam transport in a compact linear proton accelerator

D.T. Blackfield, Y-J Chen, S.D. Nelson, A. Paul

June 13, 2007

2007 Particle Accelerator Conference
Albuquerque, NM, United States
June 25, 2007 through June 29, 2007

Disclaimer

This document was prepared as an account of work sponsored by an agency of the United States Government. Neither the United States Government nor the University of California nor any of their employees, makes any warranty, express or implied, or assumes any legal liability or responsibility for the accuracy, completeness, or usefulness of any information, apparatus, product, or process disclosed, or represents that its use would not infringe privately owned rights. Reference herein to any specific commercial product, process, or service by trade name, trademark, manufacturer, or otherwise, does not necessarily constitute or imply its endorsement, recommendation, or favoring by the United States Government or the University of California. The views and opinions of authors expressed herein do not necessarily state or reflect those of the United States Government or the University of California, and shall not be used for advertising or product endorsement purposes.

INJECTOR PARTICLE SIMULATION AND BEAM TRANSPORT IN A COMPACT LINEAR PROTON ACCELERATOR*

D.T Blackfield, Y-J Chen, S.D. Nelson, A. Paul, B. Poole, LLNL, Livermore, CA 94551, U.S.A

Abstract

A compact Dielectric Wall Accelerator (DWA), with field gradient up to 100 MW/m is being developed to accelerate proton bunches for use in cancer therapy treatment. The injector must create a proton pulse up to several hundred picoseconds, which is then shaped and accelerated up to energies up to 250 MeV. The Particle-In-Cell (PIC) code LSP is used to model several aspects of this design. First, we use LSP to obtain the voltage waveform in the A-K gap that will produce a proton bunch with the requisite charge. We then model pulse compression and shaping in the section between the A-K gap and the DWA. We finally use LSP to model the beam transport through the DWA.

PROTON INJECTOR

First, we use the PIC code LSP to model the injector to the DWA. We assume an azimuthally symmetric injector, 18 cm in length. Radially, we model the central 5 cm. Figure 1 shows the 2-D geometry (r,z) that LSP uses when simulating the proton injector section. We will examine scenarios for three different voltage waveforms launched from the emission gap radial boundary (A). The anode surface (S) is shaped so that the path lengths on either side of the channel where the voltage pulse is launched are approximately equal to reduce reflections.

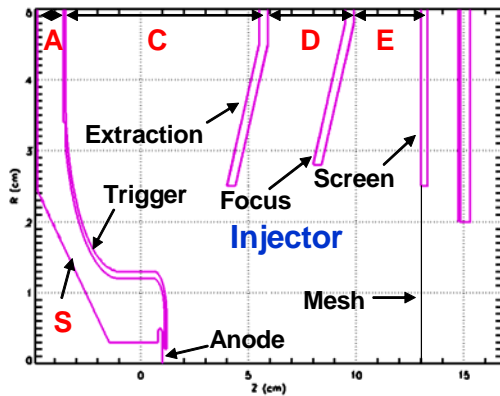


Figure 1 LSP model of the injector. The DWA begins beyond the metal mesh located at $z=13.1$ cm.

In these simulations the smallest gap occurs between the anode surface and the trigger electrode, being 1 mm. This small gap, shown in figure 2 and the assumed radius of particle emission of 1 mm on the anode surface restricts the LSP grid to 0.1 mm x 0.1 mm with a resulting time step of 0.2 ps. A metallic mesh, that shorts out the electric field while allowing particles to pass through without loss is located at $z = 1.2$ cm. We assume that both protons and electrons are created on a flat anode surface at $z = 1.0$ cm assuming Child-Langmuir emission.

Additional voltage pulses are launched at the radial boundary between the trigger and extraction electrodes (C), extraction and focus electrodes (D) and focus and screen electrodes (E). These voltage waveforms compress and shape the protons that leave the emission gap. A similar lossless metallic mesh, is located at $z=13.1$ cm, the entrance to the DWA. The LSP particle simulation data is collected at this location to be used when LSP simulates the beam dynamics of the DWA accelerator.

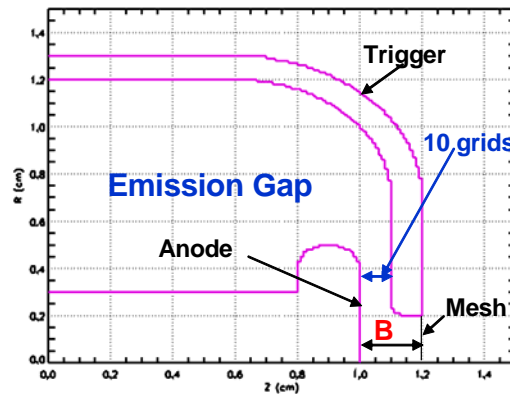


Figure 2 LSP model of the emission gap.

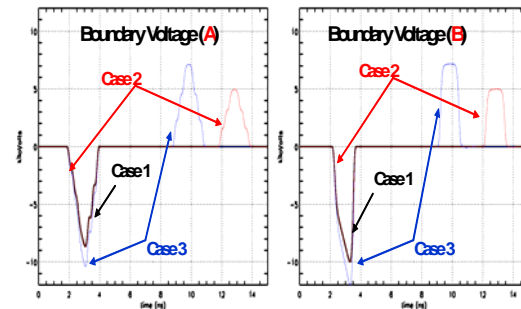


Figure 3a-b Voltages in kV at the emission gap boundary (A) and on axis in the emission gap (B).

Figure 3a show voltage ramps on the emission gap boundary for the three cases presented below. Using a transformation matrix, based on the EM pulse channel geometry, these boundary waveforms produce the desired on axis voltage waveforms, shown in figure 3b. For case 1, there is a single voltage peak centered at $t = 3$ ns with a half width of 1.5 ns. In case 2, this same voltage peak is followed about 6.0 ns later by a similar voltage peak, with opposite sign and half the peak value. For case 3, the peak values have been increased while the time between peaks has been decreased to 4.25 ns. All three cases use the same voltage ramps on the other injector electrodes. The first voltage peak causes the anode to emit protons. However, once protons occupy the emission gap, electrons are emitted from the surface. These electrons

cannot travel beyond the mesh at 1.2 cm due to the presence of a large repelling electric field produced by the voltage difference between the trigger and extraction electrodes shown below. Although electrons travel up the channel to the boundary (A) most remain in the emission gap. Without the presence of an externally supplied voltage difference in the emission gap, these gap electrons continue to pull protons from the anode surface well after the initial voltage pulse has dissipated. In case 1, there is only a single voltage pulse. In case 2, a second pulse, with opposite polarity is supplied to cutoff the continued streaming protons. In case 3, higher voltage peaks are supplied, closer in time to produce approximately the same amount of charge in the beam bunch that will eventually reach the DWA. However, in case 3, the beam bunch is shorter. The total proton flux at the metal mesh for each of the cases is shown in figure 4. Notice that the presence of the second voltage pulse removes the long tail of protons. The amount of charge and the initial bunch length can be modified by varying the two pulse heights and interval.

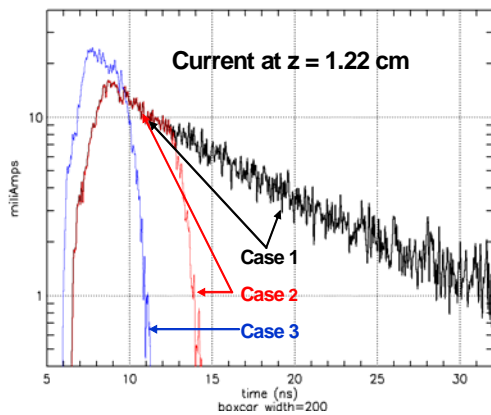


Figure 4 Total current just beyond the metal mesh.

After emitting electrons and protons in the emission gap, we next follow those protons that travel beyond the metal mesh. The average he boundary voltages between the remaining sets of electrodes in the injector region are set to focus the beam towards the end of the DWA while these electrode voltages are ramped linearly about their averaged values so that the beam will be longitudinally compressed. The C voltage difference is -610kV until 5 ns. At 5 ns it changes linearly reaching -1190 kV at 16 ns and remains at this value. The D voltage difference is 1190 kV until 10 ns where it linearly ramps to 610 kV at 19 ns and remains at this value. Finally the E voltage difference is -610 kV until 16 ns where it ramps linearly to -1050 kV at 23 ns and remains at this value. These ramps over compress the beam with later emitted protons passing earlier ones around 16.7 ns at a z location near 8.6 cm. Further refinements in electrode shapes and placements are expected to provide more optimal compression and focusing. Despite being overly compressed, the figure 5 shows that the beam pulse width has greatly decreased

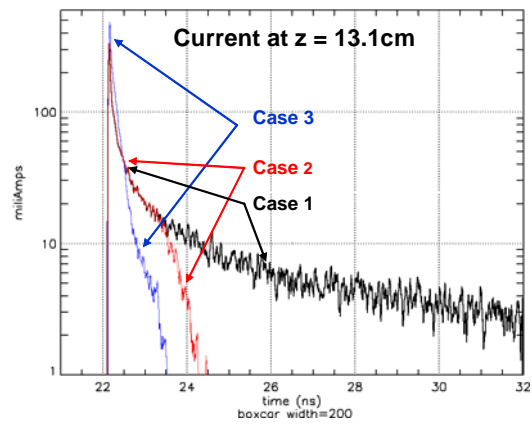


Figure 5 Total current at the end of the injector region

For case 3, the beam pulse has decreased from 5 ns to less than 2 ns with most of the current within 300 ps. The beam energy at the end of the injector is the same for Case 1 and Case 2. For Cases 1 and 2, the beam energy rises slowly from 890 to 995 keV, while for Case 3, the beam energy is flat varying from 870 to 890 keV. In the next 5 ns, for Case 1 the tail, which can contain up to 1/2 of the total charge, slowly rises to 1500 keV before leveling off around 1570 keV? In the next section we follow the Case 3 300 ps beam bunch through a subscale prototype DWA.

DWA PROTON ACCELERATOR

Our most recent simulations involve the subscale prototype DWA. We expect this machine to achieve field gradients similar to the full scale DWA but be shorter, 40 cm long. For these simulations we again used an azimuthally symmetric LSP model of a set of stacked radial transmission lines. The model begins with a conducting boundary representing the mesh at the end of the injector. Beyond this boundary, the DWA is modeled as 100 sets of 0.2 mm thick electrodes, each set separated by 3.8 mm. The radial boundary of this cylindrical model is at 3.0 cm. The wall radius is 2.0 cm. Finally there is a conducting, boundary at $z=40.4$ cm. We inject 68 pC of protons with radial positions and velocities collected on a plane at $z=13.1$ cm from Case 3. The current and energy of this bunch are shown in figure 6.

The shapes and timing of each pulse launched from the 100 outlets at the boundary are obtained from XFTD[1]. Changing the timing slightly at the boundary can have greater impact on the beam dynamics since the EM fields generated in many adjacent lines overlap within the beam tube. Besides the timing between the boundary pulses, the time when the bunch enters the DWA also has a large impact on beam dynamics. We will present two scenarios where identical pulse timings are used, but the time when the bunch first enters the DWA differs by 0.8 ns. The timing between the bunch and E_z on axis 2 mm beyond the start and 2 mm before the end of the DWA are shown in figures 7 and 8 for Case 4 and 5.

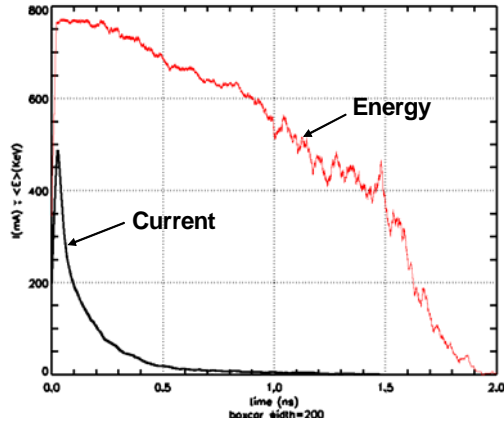


Figure 6 Injected proton current (mA) and averaged energy (keV) from Case 3.

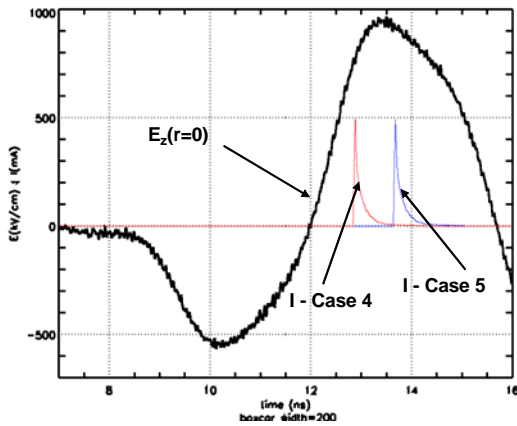


Figure 7 On axis E_z (kV/cm) and current (mA) 2.0 mm beyond the DWA entrance.

The beam may either compress or expand longitudinally; depending upon the time the beam enters the DWA. In Case 4, the bunch longitudinally compresses but radially expands as it travels through the DWA.

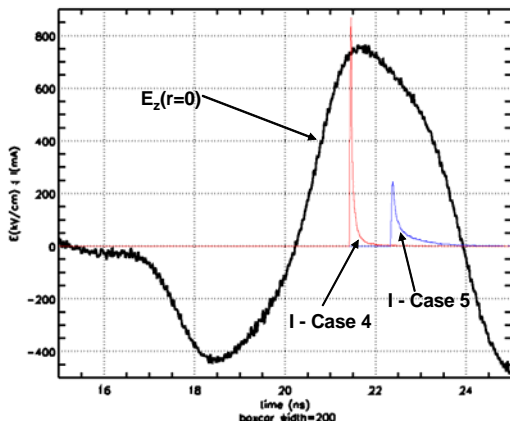


Figure 8 On axis E_z (kV/cm) and current (mA) 2.0 mm before the DWA exit.

For Case 5, the beam pulse lengthens but radially focuses as it is transported. Figure 9 show that while these

cases have similar beam energies, Case 4 has beam bunch is much shorter.

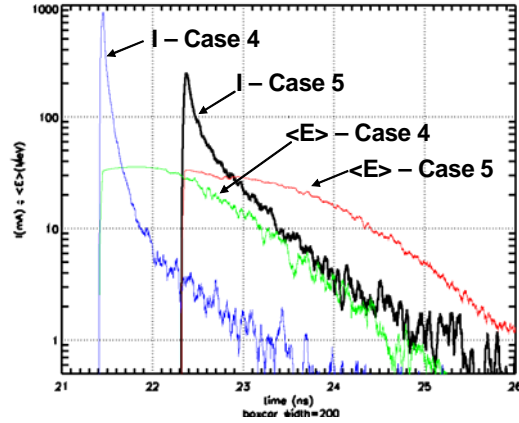


Figure 9 Current (mA) and energy (MeV) 2 mm before the subscale DWA exit.

CONCLUSION

We have simulated the transport of 300 ps proton bunches, with uniform density in r,z with a radius of 1.0 cm and an initial energy of 1.0 MeV through a 250 cm long full scale DWA[2]. We assumed that the boundary voltage pulses in all the lines had the same shape based on XFTD simulations [1]. The total charge in this bunch was 80 pC and the pulse was injected 1 cm beyond the end of the injector. At the end of the DWA, the beam energy varied from 256 to 257 MeV and while no longer uniform in density, the beam pulse had shortened to 150 ps.

We can adjust the bunch charge by varying the magnitudes and the timing between the two emission gap voltage pulses while also eliminating the electron produced ion tail. We can compress and focus this bunch by changing the remaining injector electrode voltages and ramps. Besides transporting a 68 pC proton bunch from the injector through the subscale DWA without beam loss, we can adjust the bunch shape by varying the DWA voltage pulse timing. By adjusting the timing between voltage pulses and the time when the protons enters the DWA we can longitudinally and radially compress the particle bunch as it transports through the DWA with the energy spread at the DWA exit at most a few percent. We expect that further simulations will produce a shorter more focused beam bunch.

ACKNOWLEDGEMENTS

This work was performed under the auspices of the U.S. Department of Energy by University of California, Lawrence Livermore National Laboratory under Contract W-7405-Eng-48.

REFERENCES

- [1] B. Poole, S.D. Nelson, Y-J Chen, D. Blackfield "Brian's Paper name here," PAC'07, Albuquerque, NM June 2007, p. 249, <http://www.jacow.org>.
- [2] G. Capaoraso, S. Sampayan, Y-J Chen, 2007.